ELSEVIER

Lithos 55 (2001) 139–158

LITHOS

www.elsevier.nl/locate/lithos

Raman microspectrometry of fluid inclusions

Ernst A.J. Burke *

Laboratory of Microanalysis, Faculty of Earth Sciences, Vrije Universiteit Amsterdam, De Boelelaan 1085, NL-1081 HV Amsterdam, Netherlands

Received 15 January 1999; accepted 20 March 2000

Abstract

For many kinds of fluid inclusions, the coupling of microthermometry and Raman microspectrometry is still the only viable option to obtain compositions of single fluid inclusions. A review is given on the basis of 16 years of experience and helped with about 120 references of the instrumentation, analytical conditions and methodology of the application of Raman microspectrometry to gaseous, aqueous and hydrocarbon inclusions, and their daughter minerals.

Keywords: Raman; Microspectrometry; Fluid inclusions; Daughter minerals; Review

1. Introduction

One of the major aims in the study of fluid inclusions is to obtain information on their trapping conditions. These can be determined by using isochores constructed from the molar volumes of the fluid inclusions, their composition, and equations of state for the systems concerned. The molar volume, or the density, is an essential quantity to be determined. It can be calculated or estimated using the proper phase diagrams containing data on molar volume, composition and microthermometry phase transition temperatures (ν–X–T diagrams). The procedures for obtaining the molar volumes of fluid inclusions have been described in detail for the CO_2–CH_4–N_2 system by Kerkhof (1988a,b, 1990) and by Thiéry et al. (1994). Comprehensive treatments of the study and use of fluid inclusions are given by Hollister and Crawford (1981) and Roedder (1984), and in this volume. The usual presence of several generations of fluids in a rock or ore necessitates the determination of ν–X properties of individual inclusions. Many instrumental methods have been applied to obtain analyses of single fluid inclusions (see the reviews by, e.g., Roedder, 1990; Boiron and Dubessy, 1994; Shepherd and Rankin, 1998; Shepherd et al., 1998), but for many kinds of fluid inclusions, the coupling of microthermometry and Raman microspectrometry is still the only viable option.

2. The Raman effect

Inelastic collisions with vibrating polyatomic molecules or molecular groups cause energy changes in a beam of light interacting with, e.g., fluids in an

* Tel.: +31-20-444-7345; fax: +31-20-646-2457.
E-mail address: bure@geo.vu.nl (E.A.J. Burke).

0024-4937/01/$ - see front matter
PII: S0024-4937(00)00043-8

inclusion: this is called Raman scattering. Molecular groups have a number of vibrational modes corresponding to specific energy states of the molecule. Selection rules explain whether a vibrational mode is infrared and/or Raman active; symmetrical modes give the sharpest Raman peaks. Raman scattering is a weak effect (10^{-3}–10^{-6} of the irradiated light), and thus a monochromatic laser beam is normally used to study it.

The interaction of the incident light with the vibrational modes in the sample causes losses and gains of energy in the incident beam, called Stokes and anti-Stokes scattering, respectively (Fig. 1). The energy-loss process is the most probable because there will always be more molecules in lower than in higher states, and usually only the more intense Stokes side of the spectrum is analyzed. A Stokes Raman spectrum is a plot of the intensity of the scattering vs. the energy loss, expressed in wave numbers relative to the source ($\Delta\nu$ cm^{-1}, the Raman shift), i.e., the changes in wave number compared to the incident light. The peaks in the spectrum correspond to the energies of the vibrational modes of the different species in the sample. Quantification of a mixture of species is possible if appropriate scattering efficiencies (Σ and/or σ) are known for the different peaks.

Details of the theory of Raman scattering and of its application in the earth sciences can be found in the reviews by McMillan (1985, 1989), McMillan and Hofmeister (1988) and Roberts and Beattie (1995). A handbook for practical Raman spectroscopy was published by Gardiner and Graves (1989).

3. Raman microspectrometers

Raman spectra from micrometer-sized objects within transparent samples can be obtained by coupling a research-grade microscope to a Raman spectrometer. This technical *tour de force* was first carried out in 1974, in France by Delhaye and Dhamelincourt (1975), and in the USA by Rosasco et al. (1975). The French instrument was later commercialized as the MOLE (Fig. 2) by Jobin-Yvon, a division of Instruments (Longjumeau, France).

The first Raman microspectrometers had a photomultiplier as a detector. This was initially also the

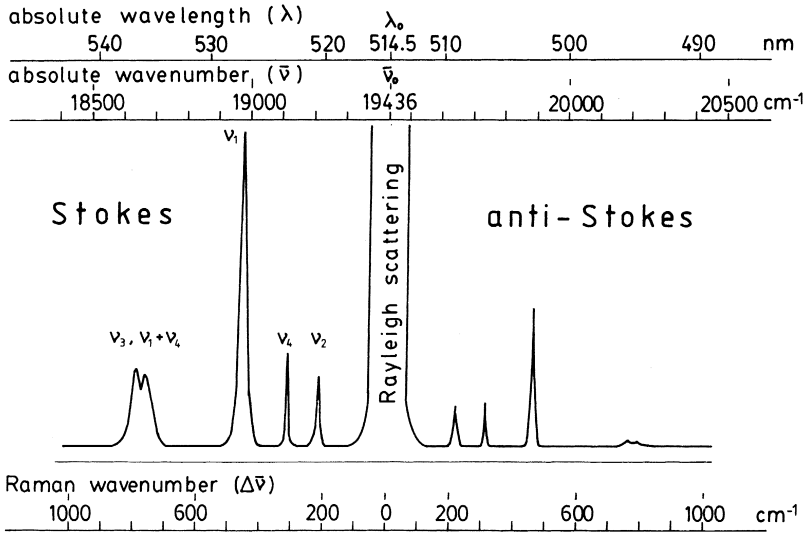

Fig. 1. The Raman effect of CCl_4, excited with 514.5 nm laser light. Most photons of the incident light are elastically scattered (Rayleigh scattering) without energy change. Some photons gain or lose a small amount of energy by inelastic scattering, resulting in pairs of Raman-shifted lines at higher (anti-Stokes) and lower (Stokes) frequencies. The Stokes lines are much more intense, and only these are normally measured. Taken from Kerkhof (1988b).

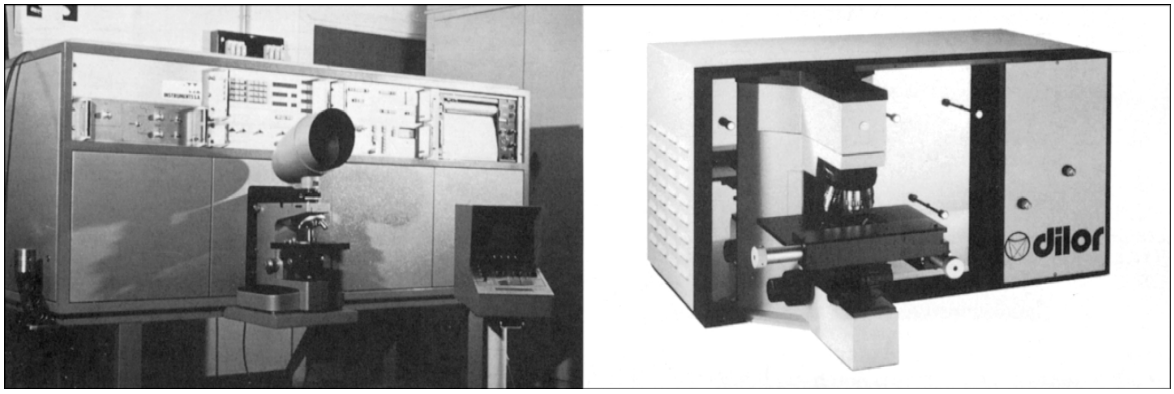

Fig. 2. Two generations of Raman microspectrometers. Left: the MOLE, the first commercial Raman microspectrometer (1976). Right: the LABRAM, the newest generation of Raman spectrometer (1997). The application in the latter of notch filters, CCD detector and confocal optics has considerably reduced the size of the instrument, but the sensitivity and the ease of use have been greatly enhanced.

case with the later Ramanor U-1000 of Jobin-Yvon. This type of monochannel scanning of spectra can be extremely slow; the analysis of a single fluid inclusion may take several hours.

Multichannel detectors were introduced in the beginning of the 1980s (e.g., Da Silva and Roussel, 1982; Purcell and Etz, 1982): an intensified photodiode array enables the recording of an entire spectrum in one event. The accumulation of many spectra gives moreover a signal-to-noise ratio increase by about one order of magnitude. The Microdil-28 of Dilor (Lille, France) was the first commercial Raman microspectrometer with a multichannel detector; such an instrument was installed in our Amsterdam laboratory in January 1984. The conventional Raman microspectrometers, using excitation in the visible range of the spectrum and a multichannel detector, are probably the ideal instruments for the study of most fluid inclusions: they produce excellent spectra in a very short time. Such instruments are available from Dilor (e.g., the XY), from Jobin-Yvon (e.g., the T64000), and from Spex (e.g., the Raman 500).

Charge-coupled devices (CCDs) have been applied for some years in these Raman microspectrometers: they offer much higher quantum yields than detectors requiring image intensifiers, two-dimensional images and exceptionally low dark current when cooled to 77 K. A CCD detector is in principle as fast as a diode array for the acquisition of a spectrum; it is, however, very sensitive to cosmic rays; an otherwise perfect spectrum can be totally ruined if a cosmic ray happens to coincide with a peak of a fluid component.

Raman microspectrometers of the newest generation (e.g., the LabRam of the Dilor component of the Instruments conglomerate, or the Systems 2000/3000 of Renishaw) are equipped with holographic notch filters for Rayleigh-line blocking, confocal configuration, thermoelectrically cooled CCD detector, air-cooled laser, and eventually a software that is able to recognize cosmic ray strikes, which then can be removed automatically from the spectrum. The use of notch filters leads to a high throughput and allows the detection of even very weak signals, and the confocal microscope optics allow to perform spatial- and depth-resolved measurements with a resolution on the micrometer scale and often strongly decreases fluorescence. With such instruments (Fig. 2) the detection of the Raman signal from fluid-inclusion components has been improved by at least one order of magnitude, resulting in a high sensitivity at very fast acquisition times.

4. Raman active species in fluid inclusions

Fluid inclusions may contain many species in the form of solids, liquids or gases. Roedder (1990) has given a summary of what to look for if the analysis of any given inclusion should be complete. Table 1 is another version of this list of wishes, adapted for Raman analysis.

Table 1
Constituents of fluid inclusions, adapted after Roedder (1990)

Liquid species (at room temperature)
Major solvents: H_2O, CO_2, H_2S
Major ions in solution: Na, K, Ca, Mg, Cl, HCO_3^-, CO_3^{-2}, HS^-, HSO_4^-, SO_4^{-2}
Minor ions in solution: Li, Al, Fe, B, Ba, Br, Mn, NH_4^-, P, F, Si
Others: *organic compounds (higher hydrocarbons, acetate, oxalate)*
Gaseous or supercritical species (at room temperature)
Major components: $^{12}\mathbf{CO_2}$, $\mathbf{CH_4}$, $\mathbf{N_2}$, H_2O
Minor components: $^{13}CO_2$, $\mathbf{H_2S}$, $\mathbf{C_2H_6}$, $\mathbf{C_3H_8}$
Rare components: $\mathbf{SO_2}$, **CO**, *COS*, $\mathbf{H_2}$, $\mathbf{O_2}$, $\mathbf{NH_3}$, *higher hydrocarbons*, He, Ar
Solid species (at room temperature)
All kinds of daughter minerals (*Raman active* and Raman inactive), see Table 3
Graphite, carbonaceous matter
Solid species (at low temperatures)
H_2O, CO_2, H_2S
Salt hydrates (e.g., of *Na, Ca, Mg, Li*)
Gas hydrates (*clathrates*) of CO_2, CH_4, N_2, and H_2S

Normal font: Raman-inactive constituents.
Italic font: Raman-active constituents, only qualitative analysis possible.
Bold font: Raman-active constituents, (semi-)quantitative analysis possible.

Only a limited number of species in fluid inclusions can be analyzed quantitatively by Raman spectroscopy, namely the polyatomic gas species and very few polynuclear species in solution. Many more species are Raman active, and their presence can be confirmed by their particular peaks in the spectrum, although for some constituents (e.g., simple cations in solution), this is only possible for their hydrates at low temperatures. Raman analysis has consequently been mainly successful for gaseous (non-aqueous volatile) components in fluid inclusions and for supercritical fluid inclusions.

The liquid phase of multiphase aqueous inclusions will generally generate only qualitative data, and then with some analytical difficulties; the gaseous phase, however, will yield quantitative results if one discounts the presence of minor amounts of water vapour (see e.g., Chou et al., 1990), because its 'peak', in reality a very broad band, is difficult to quantify by Raman microspectrometry.

5. Raman microspectrometry of fluid inclusions

The first results of Raman analyses of natural fluid inclusions were published by Rosasco et al. (1975) and Dhamelincourt and Schubnel (1977). They were quickly followed by the data of Guilhaumou et al. (1978), Rosasco and Roedder (1979) and Dhamelincourt et al. (1979); these micro-Raman pioneers not only presented a great number of possible applications of the new method to fluid inclusions, they also paved the way to the quantification of fluid mixtures by using the cross-sections (measures for the specific Raman activity of compounds) available at that time. The paper by Schrötter and Klöckner (1979), with a discussion on the cross-sections of dozens of fluid components, was a breakthrough in Raman microspectrometry, although it would take 10 years before the users of Raman analysis in the earth sciences fully understood the contents of that paper (Dubessy et al., 1989).

More comprehensive studies on fluid systems and on the method in general were then published by Bény et al. (1982) and by Touray et al. (1985), respectively. The applications of the first 'after-MOLE' Raman instruments to fluid inclusions were published by Pasteris et al. (1986) and Burke and Lustenhouwer (1987). Instrumental limitations and optimization of analytical conditions were widely discussed by Wopenka and Pasteris (1986, 1987), Seitz et al. (1987) and in particular by Pasteris et al. (1988).

The first decade of attempts at quantitative microspectrometry of fluid inclusions ended with the monumental work of Kerkhof (1988b) on the system CO_2–CH_4–N_2, and with the review by Dubessy et al. (1989), containing discussions and some necessary corrections on the analysis of C–O–H–N–S fluids.

The most recent period of Raman microspectrometry has witnessed the development of a more or less dual approach to the study of fluid inclusions. Some authors have stressed the limitations of the method and its numerous analytical uncertainties, and have pursued research to resolve all possible errors by working on synthetic inclusions and on gas mixtures of known compositions. Other authors, however, have shown on many occasions that Raman results of natural fluid inclusions, even with their obvious limi-

tations in accuracy and precision, can definitely be used to obtain important information on a great number of geological processes. This apparent kind of dichotomy should not be regarded at all as being contradictory, it is of course complementary.

6. Analytical conditions

6.1. Calibration

The $\Delta\nu$ positions of the peaks of the different species in a fluid can easily be checked by comparing them with the measured positions of neighbouring plasma lines, after removing the monochromator filter from the laser light path. Calibration of a Raman microspectrometer for the accuracy of quantitative analyses of fluids is theoretically possible if the relative Raman scattering cross-sections (the σ's) for the different fluid species are accurately known, and if the spectral efficiency of the instrument is determined (e.g., with a standard lamp). Because of the variations of the σ's with temperature, pressure and specific fluid composition (see below), and because of the lack of an effective polarization scrambler, Pasteris et al. (1988) advocated the empirical calibration of Raman microspectrometers using fluid mixtures of known composition and internal pressure.

In the absence of such standard specimens, the only empirical way to assess Raman results is to compare them with microthermometry data obtained on natural or synthetic fluid inclusions. Guilhaumou (1982) was probably the first author to do it this way, on natural inclusions of the system CO_2–N_2; Wopenka and Pasteris (1986) were the first to use this method on synthetic inclusions, in the system CO_2–CH_4. The internal consistency between fluid compositions obtained from Raman data and compositions based on microthermometry data was observed on many occasions (e.g., Andersen et al., 1989; Darimont et al., 1988; Kerkhof, 1988b), and led to confident statements about instrumental correction factors (Burke, 1989). This deceptive oversecurity was tripped up by the remarks of Dubessy et al. (1989) on the abusive use by all Raman teams of wavelength-independent relative Raman scattering cross-sections (Σ's) instead of wavelength-dependent ones (σ's). It appeared later that only compensating errors in the use of Σ's and instrumental factors kept the detriments to some Raman results within reasonable bounds (Kisch and Kerkhof, 1991; Pasteris et al., 1993; Kerkhof and Kisch, 1993).

Empirical calibrations with gas mixtures of known composition in capillaries and in sealed fused-quartz tubes were initiated by Wopenka and Pasteris (1987) and Kerkhof (1988b), respectively, and also with high-pressure-cell methods by Chou et al. (1990). The latter method was recently used for the systems CH_4–N_2 and CO_2–CH_4 (Seitz et al., 1993, 1996). The sealed fused-quartz tubes of Kerkhof (1988b) and some silica-glass tubes of Chou et al. (1990) have meanwhile been used by most Raman laboratories to calibrate the accuracy of their instruments for the analysis of fluid inclusions.

The precision (reproducibility) of Raman analyses of fluid inclusions is usually better than 5% (Kerkhof and Kisch, 1993).

6.2. Sample considerations

In order to avoid time-consuming sessions of Raman analysis on fluid inclusions which then turn out to be merely empty or just water, it is advisable to use only inclusions for which microthermometry data are available. The samples used to obtain such data, doubly polished rock wafers with a thickness between 50 and 200 μm, are in principle also perfect for Raman analysis. Such wafers should not be prepared with mounting media which readily enter the sample along cracks or fractures or which are fluorescent (see below). Our technician uses beeswax: it does not enter the sample, and it is very well soluble in white spirit or turpentine.

Some sample properties can interfere with the straightforward use of Raman analysis: an insufficiently transparent or a badly polished wafer renders the observation and/or the analysis of inclusions impossible, the 514 nm light of an argon-ion laser is absorbed by red-coloured minerals, minerals with a high refractive index (e.g., garnet or olivine) prevent the analysis of deep-seated inclusions, highly birefringent minerals (e.g., calcite) give double images at greater depths, opaque daughter minerals absorb the laser energy to a degree that an inclusion will be totally deteriorated.

Most Raman microspectrometers are nowadays equipped with high-quality microscopes (usually from Olympus) and objectives with a magnification between 50× and 150×, which allow for a laser beam diameter of 1–2 μm, or even less. Some objectives contain lenses with coatings which selectively absorb part(s) of the Raman scattering spectrum; this will lead to less accurate results.

The minimum size of fluid inclusions for Raman analysis depends on many factors: the optical properties described above, the quality of the microscope system, the available laser power, the type of detector in the spectrometer, the density (molar volume) of the fluids, the depth of the inclusions within the sample, the background signal of the matrix (e.g., usually quite high in plagioclase feldspar). Under ideal circumstances, reliable quantitative data have been obtained from inclusions as small as 2 μm situated as deep as 100 μm in quartz, e.g., the almost impossible inclusions in Fig. 4 of Fricke et al. (1990).

Even very broad and long inclusions may have a short third dimension, they can be very flat. Because of the relatively large vertical dimension of the laser focus (up to several tens of micrometers, determined by the pinhole diaphragm at the entrance of the monochromator), most of it will excite the matrix of the inclusion, not the inclusion itself. The Raman signal of such an inclusion will be weak, and moreover the slightest movement of the microscope stage, horizontally or vertically, will lead to very inaccurate results. For the same reason, all Raman peaks of the fluid components of all inclusions should be measured without changing the location or the focus depth of the laser beam; each inclusion has its own peculiar, often irregular geometry, and any change of the laser focus may have important consequences for the estimation of the volume of the inclusion excited by the laser beam. The application of a confocal configuration in the newest Raman instruments greatly improves the possibilities for measuring small inclusions.

Smaller inclusions near the surface of a sample will generally give a stronger Raman signal than larger inclusions at greater depths. Usually, one strives to analyze inclusions as near the surface as possible; inclusions deeper than 50 μm start to give problems, especially if their density is not too high. For N_2-bearing fluids, the optimum depth for analyzing inclusions is a compromise between obtaining the maximum intensity of Raman peaks and avoiding contamination from the nitrogen in the air between objective and sample: 30–70 μm. Confocal instruments have no problems with this contamination.

The vapour bubbles in two-phase inclusions in the system CO_2–CH_4–N_2 near their critical point, and in water or brine inclusions move around in the liquid; the former inclusions can be made supercritical by heating the sample slightly, and in the latter, the bubble can be driven into a corner (if the inclusion is jagged) by carefully ‘pushing’ it with the laser beam.

Weak Raman scattering from inclusions with low densities or at greater depths in a sample can be intensified by increasing the laser power or by using longer measuring times. Due to the different properties of the sample, the inclusions and the instrument will decide on the preference for a certain set of analytical conditions, preferably remaining identical for all components. The factors to be considered are as follows. Can the inclusion withstand the increased heat? How much time is needed to see Raman peaks on the computer screen? Is it possible to accumulate several spectra within acceptable time limits?

6.3. Fluorescence

The weak Raman scattering can be completely masked by fluorescence, which is several orders of magnitude stronger. Three features of the doubly polished rock wafer may cause fluorescence: the surface, the matrix mineral, and/or the fluid inclusions. Surface fluorescence may be due to incompletely dissolved remnants (even optically invisible films) of epoxy and thermoplastic resins used in the preparation of the sample, to the hydrocarbon-based ink of felt-tipped pens used to draw circles around the location of fluid inclusions to ‘help’ the Raman analyst, or simply to careless greasy fingerprints on the sample. Several minerals are well known for their fluorescence, not only fluorite, but also calcite and plagioclase feldspar, sometimes even quartz. Cracks and fractures filled with fluorescent mounting medium may prevent analysis altogether. Fluid inclusions are generally fluorescent if they contain cyclic or aromatic hydrocarbons, or fluorescent daughter minerals.

Besides using a confocal Raman instrument, there are several remedies to avoid fluorescence effects; a surface can be cleaned, fluorescence in minerals may in some cases greatly be diminished by heating the location of intended analysis with the laser beam for several minutes. Fluorescent fluid inclusions, however, generally cannot be analyzed with conventional visual Raman microspectrometry. Individual hydrocarbon inclusions can be characterized with some difficulty with conventional Raman microspectrometry (Orange et al., 1996), and with either Fourier transform infrared microspectrometry (Wopenka et al., 1990), or by near-infrared Fourier transform Raman microspectrometry (Pironon et al., 1992). In the latter cases, however, the minimum size of the inclusions is about one order of magnitude larger than for visual Raman microspectrometry. Another possibility is to use time-resolved visual Raman microspectrometry: the fluorescence effect starts a fraction of time later than the Raman effect, which can thus be recorded before the swamping of the detector.

7. Peak positions and scattering efficiencies of Raman active species

For the qualitative analysis of Raman active species (identification) in fluid inclusions, only the $\Delta\nu$ values of their characteristic peaks are necessary. Quantitative analysis of gaseous or supercritical inclusions is only possible if the spectral efficiency of the microspectrometer (= instrumental factor) and the Raman scattering efficiencies for the different components (= cross-sections, the σ's) are known to some degree of accuracy. Table 2 lists data for the $\Delta\nu$ peak positions for current species in fluid inclusions, wavelength-independent Raman scattering efficiencies (Σ's) and wavelength-dependent Raman scattering efficiencies (σ's for laser beams with $\lambda = 488$, 514 or 633 nm), along with some references for specific examples.

Different literature sources yield somewhat different numerical data for the $\Delta\nu$ positions and for their Σ values. The data for CH_4 may serve as an example. The peak position for its ν_1 vibration is given to be 2917 cm^{-1} by most authors (e.g., Schrötter and Klöckner, 1979; Fabre and Couty, 1986), but some authors (e.g., Touray et al., 1985) give 2914 cm^{-1}. The exact peak position, however, is not really relevant for qualitative purposes, and for quantitative analysis it will only be important if it is used to determine the density of inclusions or the partial pressures of their components. Schrötter and Klöckner (1979) list in their Table 4.2 the Σ values obtained in different laboratories; the six values cited for the 2917 cm^{-1} CH_4 peak at the exciting wavelengths 488 and 514 nm are, respectively, 6.8, 9.2, 8.7, and 9.1, 8.7, 9.3: their average ($\Sigma = 8.63$) has been used in Table 2.

Σ values are relative normalized differential Raman scattering cross-sections, used only for comparing results measured at different wavelengths. The calculation of a gas composition from peak areas obtained at a specific laser wavelength, on the other hand, uses σ values, relative Raman scattering cross-sections; both values are given relative to the scattering efficiency of N_2 (Σ and $\sigma = 1$). Dubessy et al. (1989) have elaborated on the necessity of using σ values, not Σ values. Schrötter and Klöckner (1979) have shown the link between Σ and σ values with their formula 4.14, a relation also cited by Dubessy et al. (1989), but rendered totally unfit for any use by the printing process which omitted the denominator in a part of the equation. The complete expression is

$$\Sigma_i = \sigma_i \left[(\nu_o - \nu_i)^{-4} / (\nu_o - 2331)^{-4} \right] \times \left[1 - \exp(-hc\nu_i / kT) \right] \quad (1)$$

in which Σ_i and σ_i are the different scattering values for a Raman shift ν_i (in cm^{-1}), ν_o is the laser wavelength used (in cm^{-1}) (20 487, 19 435, and 15 802 for 488, 514, and 633 nm, respectively), h is Planck's constant ($6.626 \cdot 10^{-27}$ erg s), c is the light velocity ($2.998 \cdot 10^{10}$ cm s^{-1}), k is Boltzmann's constant ($1.381 \cdot 10^{-16}$ erg K^{-1}), and T is the absolute temperature. All values are in cgs units because of the cm^{-1} units of wavelengths and Raman shifts.

This formula has been used to obtain the σ values given in Table 2 (with only one decimal in view of the divergent Σ values). It should be kept in mind that all these values concern low-density fluid mixtures; they are subject to changes with pressure,

Table 2
Raman shifts ($\Delta\nu$ in cm^{-1}), wavelength-independent relative Raman scattering cross-sections (Σ) and wavelength-dependent relative Raman scattering cross-sections (σ, for $\lambda = 488$, 514 and 633 nm) of common fluid species in inclusions, with some references

Species		$\Delta\nu$	Σ	σ 488 nm	σ 514 nm	σ 633 nm	Selected references
COS		857					Grishina et al. (1992)
SO_4^{-2}		983					Rosasco and Roedder (1979), Dubessy et al. (1983)
HSO_4^-		1050					Dubessy et al. (1992), Benison et al. (1998)
SO_2		1151	4.03	5.2	5.3	5.6	Clocchiatti et al. (1983), Norman, 1994
$^{12}CO_2$	ν_1	1285	0.80	1.0	1.0	1.1	Garrabos et al. (1980)
	$2\nu_2$	1388	1.23	1.5	1.5	1.6	Kerkhof and Olsen (1990)
$^{13}CO_2$	$2\nu_2$	1370		1.5	1.5	1.6	Rosasco et al. (1975), Dhamelincourt et al. (1979)
HCO_3^-		1360					Bény and Feofanov (1993)
O_2		1555	1.03	1.2	1.2	1.3	Dubessy et al. (1988), Stein et al. (1989), Savary and Pagel (1997)
CO		2143	0.90	0.9	0.9	0.9	Bergman and Dubessy (1984), Frezzotti et al. (1995)
N_2		2331	1	1	1	1	Andersen et al. (1989, 1993), Darimont et al. (1988)
HS^-		2574					Rosasco and Roedder (1979), Kerkhof (1988b)
H_2S liquid		2580					Bény et al. (1982), Dubessy et al. (1992)
H_2S in water		2590					Bény et al. (1982), Dubessy et al. (1992)
H_2S		2611	6.8	6.4	6.4	6.2	Bény et al. (1982), Kerkhof (1991)
C_3H_8		2890		18			Dhamelincourt et al. (1979), Guilhaumou et al. (1988)
CH_4		2917	8.63	7.6	7.5	7.2	Kerkhof (1987), Larsen et al. (1992)
C_2H_6		2954		13			Saliot et al. (1982), Konnerup-Madsen et al. (1979, 1985)
H_2O liquid[a]		3219					Chou et al. (1990), Dubessy et al. (1992)
NH_3		3336	6.32	5.0	5.0	4.6	never reported
H_2O vapour[a]		3657	3.29				Chou et al. (1990), Dubessy et al. (1992)
H_2		4156	3.54	2.3	2.3	2.0	Dubessy et al. (1988), Peretti et al. (1992), Savary and Pagel (1997)

$\Delta\nu$ values from different sources; Σ's are the average values of the data cited by Schrötter and Klöckner (1979) for $\lambda = 488$ and 514 nm; σ's calculated from Σ's with their formula 4.14 (formula 1 in this text).
[a]Broad bands of several hundred cm^{-1}.

temperature and chemical composition of fluid inclusions (see below). Particular attention should be given to the variations in the Fermi diad of the Raman spectrum of CO_2: the intensity ratio of the two peak areas (usually called $2\nu_2$ at 1388 cm^{-1} and ν_1 at 1285 cm^{-1}) varies with density, but the sum of the two peak areas remains constant (Garrabos et al., 1980). According to Dubessy et al. (1989),

CO_2 concentrations in a mixture of gases should thus always be calculated using the sum of the peak areas and the sum of their σ's (e.g., 2.5 using a 514 nm laser beam). But data obtained by Seitz et al. (1996) on mixtures of CO_2 and CH_4 indicate that the peak area ratio between CH_4 and the sum of the CO_2 Fermi diad varies continuously as a function of pressure: Seitz et al. (1996) therefore conclude that it is advantageous to use only the $2\nu_2$ peak rather than the sum of the two CO_2 peaks for determining fluid composition in CO_2–CH_4 mixtures.

A simple formula based on Placzek's polarizability theory can then be applied to derive a quantitative analysis in molar fractions of species present in a fluid inclusion (Schrötter and Klöckner, 1979; Wopenka and Pasteris, 1986, 1987; Dubessy et al., 1989)

$$X_a = [A_a/(\sigma_a \zeta_a)]/\Sigma[A_i/(\sigma_i \zeta_i)] \quad (2)$$

in which X_a, A_a, σ_a and ζ_a are, respectively, the molar fraction, the peak area, the Raman cross-section and the instrumental efficiency for species a; A_i, σ_i and ζ_i represent the appropriate values for all species present in the inclusion; here, Σ is the sum. The peak areas should of course be normalized for laser power and for exciting time. An example: Raman analysis (with a multichannel detector, 600 mW laser power with $\lambda = 514$ nm, and an exciting time of 2 s per spectrum) of a single-phase (at 25°C) supercritical fluid inclusion yields a spectrum with peak areas of CO_2 at ~ 1388 cm^{-1} (4386 counts) and at ~ 1285 cm^{-1} (2580 counts), of N_2 at ~ 2331 cm^{-1} (314 counts), and of CH_4 at ~ 2917 cm^{-1} (9834 counts). The respective σ values for CO_2, N_2 and CH_4 are 2.5 (sum of two peaks), 1 and 7.5; the respective instrumental efficiencies (ζ values, calibrated with synthetic gas mixtures) for the spectrometer positions of CO_2, N_2 and CH_4 are 0.5, 1 and 1. This leads to the following reduced peak areas

$$CO_2: [(4386 + 2580)/(2.5 \times 0.5)] = 5572.8$$

$$N_2: [(314)/(1 \times 1)] = 314$$

$$CH_4: [(9834)/(7.5 \times 1)] = 1311.2$$

leading to a result (in percent) of ~ 78 mol% CO_2, ~ 4 mol% N_2 and ~ 18 mol% CH_4, based on the assumption that the low-density σ values can be applied to a fluid with an obviously higher density.

8. Modifications of Raman peaks of gases

The $\Delta\nu$ values in Table 2 for the gaseous species are only valid for low-density environments. Long before the era of microspectrometry, it was common knowledge that Raman peaks of gases are downshifted several cm^{-1} with increasing pressure or density. This fact was also observed in the very first publication on Raman microspectrometry (Rosasco et al., 1975): the 2914 cm^{-1} peak position of CH_4 (a downshift of 3 cm^{-1} from its position at atmospheric pressure) in an inclusion with CO_2 and N_2 was attributed to both pressure and solution effects. Dhamelincourt et al. (1979) tried to quantify the influence of the pressure on the ν_1 vibration peak of CH_4 by measuring its position in an almost pure CH_4 fluid inclusion at different temperatures: they observed a downshift from 2916 cm^{-1} at 1 bar to 2912 cm^{-1} at 70 bar. Fabre and Couty (1986) studied the modifications of the CH_4 peak between 1 bar and 3 kbar: they found a downshift from 2916 cm^{-1} at 1 bar to 2910 cm^{-1} at 3 kbar, and an increase in the half-height width from 0.35 cm^{-1} at 1 bar to 6 cm^{-1} at 3 kbar. Garrabos et al. (1980) documented the variations with pressure of the CO_2 Fermi diad ν_1 and $2\nu_2$ peak positions (downshifts of 5 and 3 cm^{-1}, respectively), the spacing between them, and their peak area ratio. Wang and Wright (1973) determined a maximum downshift of the N_2 peak of 3 cm^{-1} and a decrease of its half-height width with increasing pressure.

Kerkhof (1988b) summarized his downshift findings on the Raman peaks of CO_2, CH_4 and N_2 in fluid inclusions; his results on natural fluids agree well with those obtained in the studies cited above. In all one-component (unary) systems, the Raman peak position can be used to derive to some extent the density of fluid inclusions, although densities derived from homogenization temperatures during microthermometry are generally much more accurate because of the relatively small downshift values of the Raman peaks and the rather low precision of their position measurement.

Rosso and Bodnar (1995) carried out a detailed characterization of the effects of temperature and density on the Raman spectrum of CO_2, and investigated the detection limits of CO_2 in fluid inclusions

with Raman spectroscopy. In fluid inclusions of low bulk density and/or low bulk CO_2 concentration, CO_2 homogenizes to the vapour phase. In microthermometry, this can only be measured with poor precision, but CO_2 densities in fluid inclusions containing a homogeneous, free CO_2 phase can be determined to a precision of about ± 0.02 g/cm^3 using the ν_1–$2\nu_2$ peak separation in the Raman spectrum.

Extreme pressure conditions are present in the superdense CO_2 inclusions (Kerkhof and Olsen, 1990; Frezzotti et al., 1992): they may be recognized from their Raman spectra, which have both peaks shifted, an increased distance between the two peaks, an increased $2\nu_2/\nu_1$ peak intensity ratio, broadened peak bases, and flattened 'hot bands' (Fig. 3).

Chou et al. (1990) and Seitz et al. (1993) have studied the behaviour of Raman peaks within the binary system CH_4–N_2. For pure CH_4 and N_2, they found the same results as Fabre and Couty (1986) and Wang and Wright (1973). For mixtures of the two components they observed that a number of peak parameters (position, height, half-height width, area, shape) do not only change with pressure, but also with composition (kind and amounts of other gas species). Chou et al. (1990) and Seitz et al. (1993) were able to quantify a number of the peak modifications in terms of composition and pressure, although only for a limited range of conditions. Their data, however, are of great value as the system CH_4–N_2 is poorly described from the microthermometric point of view. Notwithstanding all the observed peak modifications, it should also be very comforting for the routine Raman analyst that the peak area ratios (the classical parameter used to determine molar proportions in a gas mixture, see above) for different CH_4–N_2 mixtures remain constant above 75 bar, and up to at least 3 kbar (as confirmed by Fabre and Oksengorn, 1992), and also that the *F*-factor (a combination of the scattering and instrumental efficiencies) ratios do not change with composition.

Seitz et al. (1996) have carried out a similar study within the binary system CO_2–CH_4 at pressures up to 700 bar and room temperature. Also here, several peak parameters are sensitive to composition and/or pressure of the fluid mixtures, and the magnitude of the observed shifts and changes is sufficient to be useful as monitors of fluid pressure and/or fluid composition. In this system the peak area ratios and the *F*-factor ratios for different mixtures also remain constant, but only above 150 bar, and only for the upper Fermi diad member (usually called the $2\nu_2$ peak) of CO_2, this in contrast to data from other authors (see above).

Data for peak modifications in the binary system CO_2–N_2 or in ternary systems are not yet available.

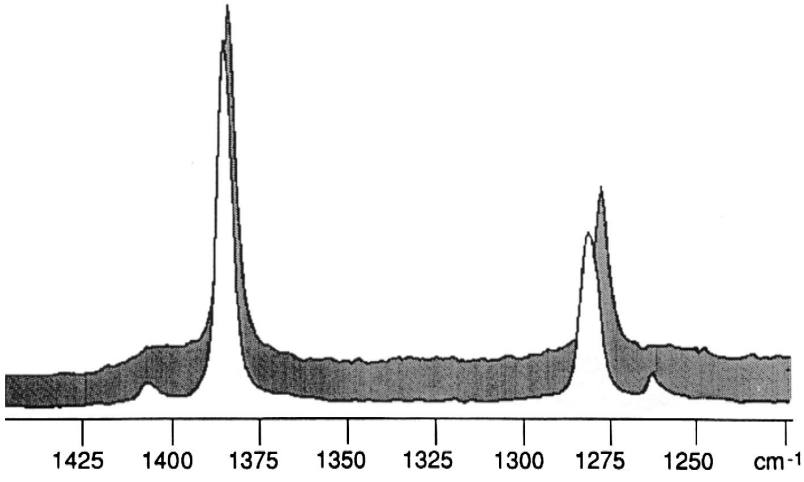

Fig. 3. Influence of internal density on the Fermi diad of CO_2. Raman spectra of a superdense inclusions ($d = 1.21$ g/cm^3) in clinopyroxene in a mantle xenolith from Oahu (black), and of an inclusion ($d = 0.7$ g/cm^3) in quartz from Switzerland (white). Spectra are plotted on the same vertical and horizontal scales. The shift with pressure increase of the ν_1 peak is greater than for the $2\nu_2$ peak. Taken from Frezzotti et al. (1992).

9. Variations in Raman cross-sections of gases with density

The Σ and σ values for gases in Table 2 have been determined in low-density fluids. This implies that variations of σ's are not very important for fluids with low vapour-like densities. At higher densities molecular interactions are much stronger, and the σ's should eventually be corrected. Dubessy et al. (1989) have shown, however, that the internal field effect at higher densities is negligible, and that of the other possible molecular interactions only the Fermi resonance correction for CO_2 should be applied (see above).

Pasteris et al. (1988) have theoretically evaluated that the ratio of the σ's for CO_2 and CH_4 and the ratio of their instrumental factors should remain unchanged between 1 and 80 bar. They observed nevertheless important differences between the σ ratios for CO_2–CH_4 mixtures at <15 and 80 bar. The data of Pasteris et al. (1988), also reported by Seitz et al. (1987), however were obtained on fluid inclusions containing not only CO_2 and CH_4, but also H_2O, and the compositions of the inclusions were inferred from microthermometry. The presence of clathrate, especially of CO_2, may thus have influenced the microthermometry T_mCO_2 and T_h readings. The erroneous character of these σ data was reported by Seitz et al. (1996), but these authors could indeed confirm that, in H_2O-free CO_2–CH_4 mixtures, the ratio of the peak areas of the components is sensitive to pressure below 100 bar. The data of Seitz et al. (1993), obtained on synthetic CH_4–N_2 mixtures in high-pressure tubes, show similar changes of σ ratios between 1 and 75 bar: it means that molecular interactions could indeed be significant in this pressure interval.

10. Special features of gaseous inclusions

10.1. Presence of $^{13}CO_2$

The Raman spectrum of CO_2 usually contains four peaks: the Fermi resonance diad with the ν_1 peak at ~ 1285 cm^{-1} and the $2\nu_2$ peak at ~ 1388 cm^{-1}, and the two 'hot bands' on the outsides of the Fermi diad at ~ 1265 and ~ 1410 cm^{-1}, respectively (see white spectrum in Fig. 1; also Figs. 4 and 5). Many inclusions produce an additional peak on the inside shoulder of the $2\nu_2$ peak, at ~ 1370 cm^{-1} (Fig. 4). This peak is due to the $2\nu_2$ vibration of $^{13}CO_2$; it is generally of quite low intensity, and common irregularities in the shoulder of the much larger $2\nu_2$ peak of $^{12}CO_2$ impede its quantification. Rosasco et al. (1975) give a possible precision of

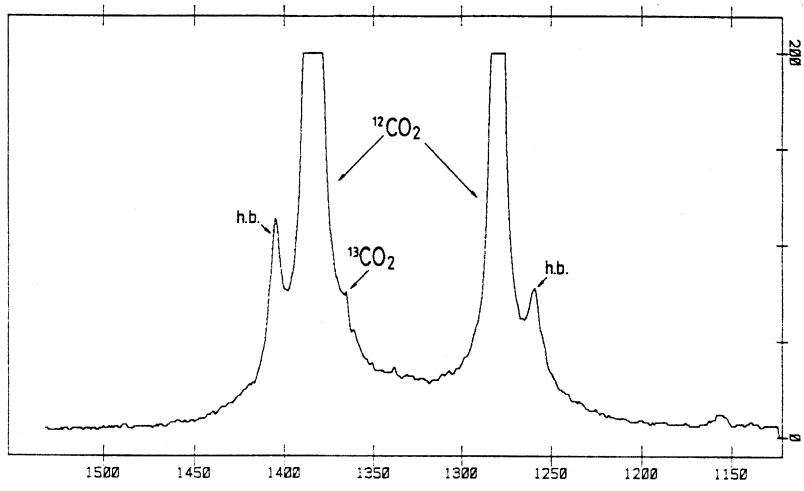

Fig. 4. Enlarged part of a CO_2 spectrum to enhance the small $^{13}CO_2$ peak; hb: hot bands. Taken from Kerkhof (1988b).

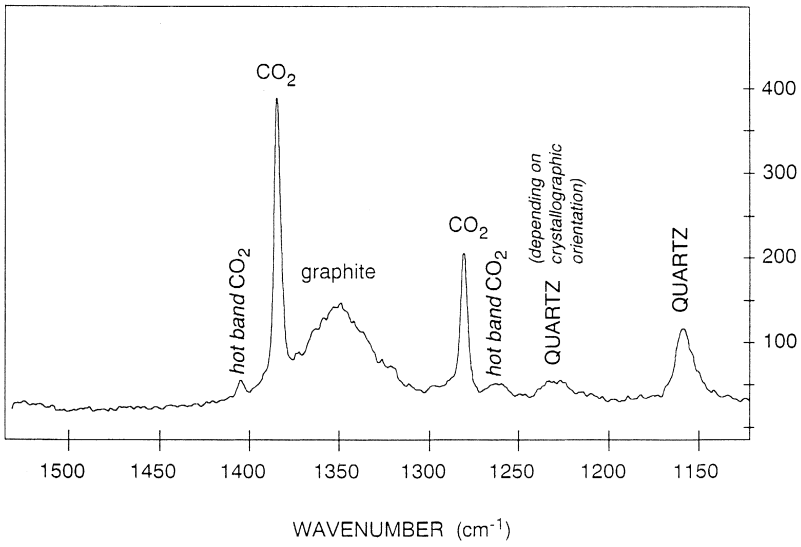

Fig. 5. Crowded spectrum around the CO_2 Fermi diad: the spectrum contains peaks of quartz at 1160 and 1230 cm^{-1}, and the peak of disordered graphite at 1350 cm^{-1}.

20‰ and Dhamelincourt et al. (1979) of only 37‰ for the determination of $\delta^{13}C$. The newest generation of Raman instruments and detectors should be able to improve considerably the precision of this potentially interesting application of Raman analysis.

10.2. Reactions in inclusions

The heat-energy of the laser beam is normally not transmitted to fluid inclusions: two-phase CO_2 inclusions near their critical point at room temperature are as a rule not homogenized by the laser irradiation. Rosso and Bodnar (1995) have shown that laser-induced heating of the molecules in the excitation volume is not significant. Things may change drastically, however, if the inclusions contain particles (not necessarily visible through the microscope, even at higher magnifications) which will absorb the laser light: a complete deterioration or burnout then follows rapidly.

Sometimes the outcome of a reaction within an inclusion may be seen. Rosasco et al. (1975) describe a phenomenon which can be observed regularly in inclusions containing CH_4 and higher hydrocarbons: the precipitation of opaque material due to the polymerization of organic constituents.

A special reaction takes place in CO_2–CH_4 inclusions with suitable mixtures of the components, between 30–70% and 70–30% (Kerkhof, 1988b; Kerkhof et al., 1991). Such CO_2–CH_4 compositions should be incompatible in many high-density inclusions at room temperature (Kreulen, 1987), they should react following

$$CO_2 + CH_4 \rightarrow 2H_2O + 2C \quad (3)$$

but the forming of graphite may be delayed by its high nucleation energy. The presence of tiny opaque particles may result in a local temperature rise triggering the reaction, which uses equal amounts of both components from the gas phase, and which will proceed until the total consumption of the lesser component. The build-up of Raman spectra of CO_2–CH_4 inclusions should be monitored closely during their acquisition in order to notice an eventual reaction and to avoid obtaining totally wrong molar fractions.

The graphite-forming reaction does not always proceed, even when graphite particles are already present: during measurements on a series of 55 inclusions (CO_2–CH_4–H_2O–C) in quartz from a shear zone in Zimbabwe only two inclusions reacted, perhaps due to the presence of water, which could

conduct the heat (Huizenga and Touret, 1999). As a rule, solids in 'dry' vapour-phase inclusions will be influenced much faster by the laser heat than solids in 'wet' liquid-phase inclusions.

Seitz et al. (1996) have observed another photochemical reaction in silica-glass tubes filled with mixtures of CO_2 and CH_4: the formation of yellowish droplets (aromatic hydrocarbons?) that strongly fluoresced under the laser beam.

10.3. Interference from Raman lines of external components

The small size of most fluid inclusions (usually < 20 μm, often < 10 μm) and the large vertical dimension of a laser beam focus (usually > 20 μm) in nonconfocal instruments may cause the presence of Raman lines of the enclosing mineral in the spectra of fluids. CO_2 spectra obtained with multichannel or CCD detectors from small inclusions in quartz always contain the $\Delta\nu = 1160$ cm^{-1} peak of quartz. This line does not interfere at all with the CO_2 lines, on the contrary, it provides some kind of reassurance that the instrument is working properly when the CO_2 peaks are absent for some reason (CO_2 density too low, no CO_2 at all in the inclusion, or even worse, the laser beam is positioned outside the inclusion).

Most Raman microspectrometers are operated with monochromator slits of 100 or 200 μm, giving a rather low spectral resolution of only 3–6 cm^{-1}. This could be a problem for the detection of SO_2 (peak at ~ 1151 cm^{-1}) in inclusions in quartz (peak at 1160 cm^{-1}), and is perhaps the reason for only one literature reference for natural SO_2 inclusions (Clocchiatti et al., 1983), although the presence of SO_2 in inclusions cannot be considered as rare (Norman, 1994). As a matter of fact, the conflicting results of microthermometric and Raman analyses in CO_2 fluid inclusions reported by many authors (e.g., Frezzotti et al., 1992) from mantle xenoliths have been solved by the identification, with the newest generation of very sensitive Raman microspectrometers, of small amounts of SO_2 in these inclusions.

Interference from atmospheric N_2 cannot be avoided if inclusions are situated very near the top surface of a sample (less than 20 μm). This problem can be solved, either by directing a flow of some other gas (e.g., argon) between the specimen and the microscope objective, or by using immersion (water or non-fluorescent oil) objectives. Both methods, however, have more drawbacks than benefits: the extremely tiny pieces of wafers (broken up for microthermometry purposes) must be fastened to the carrying glass slide to prevent it from blowing away or from sticking to the front lens of the objective. Blank measurements outside the inclusions, at the same focus depth, can be used to correct for eventual atmospheric contributions. Atmospheric N_2 and denser N_2 from inclusions can be discriminated by the peak shift for the inclusion N_2.

Particularly difficult is the analysis of N_2- and/or CO_2-bearing inclusions in cordierite having the channels in its structure filled with N_2 and/or CO_2 (Winslow et al., 1991; Herms and Schenk, 1992). Fluids in the inclusions and fluids incorporated in the mineral can be discerned by the greater peak shifts of N_2 and CO_2 in cordierite, but quantitative analysis of inclusions in such a matrix is impossible.

11. Aqueous inclusions

Aqueous inclusions may contain many species, considerably more than gaseous inclusions (Table 1). Raman data are available for a number of polyatomic anions, but Dubessy et al. (1989, 1992) have shown that PO_4^{-3} concentrations are usually very low in geological fluids, that NO_3^- is an unstable species, that CO_3^{-2} only occurs at unrealistically high pH conditions, and that HCO_3^- is a low Raman scatterer hidden by Raman bands of quartz and calcite. The latter statement, however, has been contradicted by Bény and Feofanov (1993), who found a peak of HCO_3^- at 1360 cm^{-1}. Only HSO_4^-, SO_4^{-2} and HS^- (H_2S in water) have been identified and also been quantified, e.g., for pH determination (Rosasco and Roedder, 1979; Dubessy et al., 1983, 1992; Murata et al., 1997; Benison et al., 1998; Boiron et al., 1999); their Raman data have been included in Table 2.

The salinity of aqueous solutions (expressed in NaCl eq. wt.%) in fluid inclusions is commonly determined by microthermometry, but several features may cause difficulties: metastability of solutions, clathrate formation, stretching of inclusions by

ice formation. Mernagh and Wilde (1989) have used skewing parameters of Raman spectra of aqueous solutions at room temperature to determine their total salinity, although this method is subject to important errors, especially if high concentrations of anions other than Cl^- are present.

The monoatomic cations in aqueous solutions can only be identified by Raman analysis from measurable crystals of their salt hydrates which form on cycled cooling down to $-170°C$. Dubessy et al. (1982, 1992) have presented reference spectra for the synthetic salt hydrates of Li, Na (hydrohalite), K–Mg (carnallite), Ca (antarcticite) and Fe. But the identification of individual salt hydrates in natural fluid inclusions containing several cations is not easy and simple at all. Mernagh and Wilde (1989) reported a number of overlapping bands, which prevented any identification, and Winter and Roberts (1993) could not match the Raman peaks of their hydrates with those for synthetic end-member hydrates as the natural fluids are likely to produce mixed hydrates, or hydrates of different stoichiometries, a fact also noticed by Grishina et al. (1992).

12. Aqueous / non-aqueous inclusions

The vapour phase in 'aqueous–carbonic' inclusions may contain the same non-aqueous volatile species as gaseous inclusions, notably CO_2, N_2, CH_4 and H_2S. Quantitative determinations with Raman spectrometry of such inclusions meet with two major problems: H_2O is a very poor Raman scatterer, and at ambient temperatures these inclusions contain multiple phases, with H_2O and the other volatiles of interest occurring in different phases. The estimation of the volume proportions of each phase at room temperature is often necessarily inaccurate, and therefore Raman analysis of such inclusions above their homogenization temperature is the indicated way to obtain reliable data on their bulk composition and density properties. Attempts to quantify these mixed inclusions (after homogenization by heating) have until now been carried out only on synthetic inclusions, and have been published in conference abstracts for the systems $H_2O–CO_2$ (Bodnar et al., 1996) and $H_2O–CH_4$ (Leng et al., 1998), and in a major paper by Dubessy et al. (1999) for the system of $H_2O–CO_2–CH_4$. The main conclusions of the latter paper are that molecular interactions are stronger between CO_2 and H_2O molecules than between CH_4 and H_2O molecules, and that for water-rich fluids the ratio of Raman scattering cross-section of CH_4 and H_2O does not vary to a wide extent, showing that the calibration of this ratio is feasible for an analytical purpose.

Upon cooling, the non-aqueous volatiles form solids by combining with H_2O. These gas hydrates are called clathrates, ice-like host-guest systems containing guest molecules (the gases) in cages of hydrogen-bonded water molecules. Raman spectra of clathrate hydrate guest molecules for different structures in several systems have been presented by Sum et al. (1997). Clathrates can easily be identified from their Raman spectra at low temperatures ($-140°C$): the clathrates of CH_4, N_2 and H_2S have two Raman peaks, respectively, ~ 10 and ~ 20 cm^{-1} lower than their gaseous Raman shifts (e.g., for CH_4 at ~ 2910 and ~ 2899 cm^{-1}), whereas CO_2 clathrate has only a downshift of ~ 10 cm^{-1}, but for each of the Fermi diad peaks, thus at ~ 1378 and ~ 1276 cm^{-1}.

On their formation, clathrates are not necessarily visible under the microscope, even at higher magnifications. This fact, and an eventually variable partitioning of gases into clathrates during cooling, may lead to significant errors in the estimation of the composition of the gas phase of such inclusions. Murphy and Roberts (1993, 1995, 1997) have shown that preferential partitioning of CO_2 into the clathrate will result in a significant depression of $T_m CO_2$, and hence will lead to an overestimation of the other volatile species present (CH_4, N_2 and/or H_2S). The ν–X properties of fluid inclusions containing clathrates can be calculated with computer programs by Bakker (1997).

13. Hydrocarbon inclusions

Organic fluids in rocks include hydrocarbons ranging from methane to high-molecular-weight hydrocarbons. Raman spectroscopic studies of hydrocarbon-rich inclusions are very few in number because such studies are generally deemed to be very difficult or impossible. The reasons for this opinion

are: (1) the usual presence of laser-induced fluorescence from many natural hydrocarbons and their host minerals; (2) the laser-induced degradation of such inclusions; (3) the very low Raman signal obtained from the necessarily low laser power which can be used on such inclusions. But e.g., Guilhaumou (1982), Guilhaumou et al. (1988) and Pironon (1993) have shown that Raman studies on hydrocarbon fluid inclusions are possible in spite of the obvious problems and difficulties. Orange et al. (1996) have carried out a successful Raman feasibility study on hydrocarbons by combining an appropriate selection of the laser excitation line (the 633 nm light of a He–Ne laser) with a minimization of the excitation volume of fluorescence (low laser power and long integration times). This technique, however, remains qualitative because of complications associated with the quantification of the Raman cross-sections.

Raman spectra and cross-sections of selected hydrocarbons are given by Stephenson (1974).

14. Daughter minerals

Raman spectroscopy of solids started immediately after the discovery of the effect in 1928, but almost 50 years later, Griffith (1974) stated in a review that 'the use of Raman spectroscopy for characterization and for structural studies of minerals is at present in its infancy'. At that time,Raman spectra of only about 100 minerals had been reported. This situation has been improved during the last 25 years for the identification of daughter minerals in fluid inclusions. Nowadays, spectra of several hundred minerals have been presented, but there is still much to be done, and in contrast to the situation for infrared data there is no comprehensive catalogue available with Raman spectra of minerals.

Several problems frustrate the forthright substantiation of solid phases in general and in fluid inclusions in particular. Many minerals (the majority?) containing rather weak bonds or bonds of strongly ionic character (e.g., halogenides as NaCl and KCl, very important for inclusions) have only weak Raman spectra, or no spectra at all. The polarized nature of the laser beam causes important differences in the spectra with the orientation of the crystal, in peak intensities and also in peak positions. In solid solutions, the peak position depends on the chemical composition of the mineral (e.g., garnets, amphiboles).

Reviews on Raman spectroscopy of minerals with their spectra and/or their sources have been published by Griffith (1974, 1975, 1987), White (1975), McMillan and Hofmeister (1988) and recently by Pinet et al. (1992). There is also a Caltech website with hundreds of Raman spectra of minerals athttp://minerals.gps.caltech.edu/files/.

14.1. Host minerals

Fluid inclusions are usually studied in only a limited number of minerals. The recognition of minerals in the thick doubly polished rock wafers is often very difficult, and therefore the main lines in their Raman spectra are given here. The strongest peak of quartz is at 466 cm^{-1}; relatively strong lines occur also at 128, 206, 1082 and 1160 cm^{-1}, and a weak band at $\sim$1230 cm^{-1}, strongly orientation-dependent, is near the CO_2 spectrum (Fig. 5). Calcite has a very strong line at 1085–1086 cm^{-1}, and lesser peaks at 156, 283 and 711 cm^{-1}; the lower peaks are important to distinguish the mineral from aragonite, which has its peaks at 152 and 209 cm^{-1} (Table 3). Fluorite has only one weak line (at 322 cm^{-1}) when it is pure CaF_2, but Burruss et al. (1992) have shown that the rare-earth elements (REE)

Table 3
Main Raman shifts ($\Delta\nu$ in cm^{-1}) of peaks used to identify the most common Raman-active daughter minerals in fluid inclusions. Data from several sources, with numerical values subject to differences of several cm^{-1}

Carbonates						
Aragonite	152	209	710	1089		
Calcite	156	283	711	1085		
Mg-calcite	157	284	714	1087		
Magnesite		329	738	1094		
Dolomite	176	299	725	1097		
Nahcolite			684	1046	1266	
Sulphates						
Anhydrite	515	628	674	1015		
Gypsum	492	623	671	1006	3250	3500
Barite	460			988		
Phosphate						
Apatite				966		

cause many peaks, attributable (even quantified) to individual REE. Silicates are generally rather weak Raman scatterers, but some host minerals of fluid inclusions have sufficiently strong peaks (some even very intense) to allow for their identification. Feldspar has two peaks at ~475–480 and ~510 cm^{-1}, olivine has two strongly orientation-dependent peaks at ~825 and ~865 cm^{-1}, pyralspite garnets have a single strong peak between 905 and 920 cm^{-1}, and ugrandite garnets between 875 and 890 cm^{-1}. Pyroxenes have only weak peaks at ~1015 and ~675 cm^{-1}, amphiboles very weak peaks at ~1050 and 1030 cm^{-1} and a better one at ~670 cm^{-1}.

14.2. Daughter minerals

The identification of daughter minerals in fluid inclusions by Raman analysis has been most successful with species having polyatomic anions containing strong bonds between oxygen and the central cation, e.g., carbonates, sulphates and phosphates. The Raman peaks of these bonds are so strong that even tiny submicrometer particles can be identified without problems. Table 3 presents the main Raman lines for the most common Raman-active daughter minerals. As already mentioned above, the even more common halogenide daughter minerals are generally Raman-inactive, or have extremely weak lines. Their hydrates, or other H_2O-bearing halogenides may eventually be identified (see above).

The carbonates in Table 3 can easily be distinguished, even if their peaks are almost in the same position. The three crystalline forms of calcium carbonate (calcite, aragonite, vaterite) have different Raman spectra, allowing their discrimination (Truchet et al., 1995). The frequent occurrence of the bicarbonate nahcolite (first described from inclusions by Dhamelincourt et al., 1979) has been confirmed by e.g., Darimont et al. (1988) and by Andersen et al. (1989). Bischoff et al. (1985) have shown that the controversial Mg-calcite has a much broader peak base than pure calcite, even at relatively low $MgCO_3$ contents; this feature has been used by Ting et al. (1994) and by Burke (1998) to discern both calcite and Mg-calcite as daughter minerals in carbonatites.

More exotic daughter minerals have been described by Raman microspectroscopy, e.g., native sulphur (Bény et al., 1982), hematite (Dhamelincourt et al., 1979), parisite (Rosasco and Roedder, 1979), glauberite (Dubessy et al., 1983), aphthitalite and görgeyite (Hansteen and Burke, 1990), ferropyrosmalite (Dong and Pollard, 1997), and burbankite (Bühn et al., 1999). The identification of sulphides in fluid inclusions and especially in melt inclusions has been made possible by the work of Cervelle and Moëlo (1990) and especially of Mernagh and Trudu (1993) and Mernagh and Hoatson (1995), but very low laser power should be used in order to prevent 'oxidation' of these phases and their surroundings.

The presence of graphite or graphitic material (carbonaceous matter) in carbonic fluid inclusions is very important for a number of interpretative parameters. The particles of this material may be so tiny that they are invisible, inclusions containing them may appear totally clear. But the Raman spectrum of graphite and carbonaceous matter is so strong that it will be rarely missed. Perfectly crystalline graphite has only one Raman line, at ~1580 cm^{-1}. Most natural graphite has, however, some degree of disorder causing a second line at ~1350 cm^{-1}. The latter line interferes with the CO_2 spectrum (Fig. 5). The 1350 cm^{-1} line may even be stronger than the 1580 cm^{-1} line in some specimens of carbonaceous matter. Wopenka and Pasteris (1993) have elaborated on the use of Raman spectra of this material for geological purposes; further examples of this application of Raman spectroscopy were given by Frezzotti et al. (1994), Andersen and Burke (1996), and Cesare and Maineri (1999). Luque et al. (1998) have described the similarities and differences between metamorphic graphite (formed in situ from organic matter) and fluid-deposited graphite.

Acknowledgements

Jacques Touret was the forward-looking initiator for the installment of a Raman microspectrometer in Amsterdam in January 1984; he enticed me to start a second career in the earth sciences. I am particularly grateful to the dozens of researchers who came to Amsterdam to obtain Raman analyses of their fluid inclusions; these data have been used for the publication of about 30 PhD theses and of about 130 papers. Raman microprobe facilities were provided by the Vrije Universiteit Amsterdam and by NWO, the

Netherlands Organization for Scientific Research. Reviews by Curt Broman and Fernando Corfu are greatly appreciated.

References

Andersen, T., Austrheim, H., Burke, E.A.J., Elvevold, S., 1993. N_2 and CO_2 in deep crustal fluids: evidence from the Caledonides of Norway. Chem. Geol. 108, 113–132.

Andersen, T., Burke, E.A.J., 1996. Methane inclusions in shocked quartz from the Gardnos impact breccia, south Norway. Eur. J. Mineral. 8, 927–936.

Andersen, T., Burke, E.A.J., Austrheim, H., 1989. Nitrogen-bearing, aqueous fluid inclusions in some eclogites from the Western Gneiss Region of the Norwegian Caledonides. Contrib. Mineral. Petrol. 103, 153–165.

Bakker, R.J., 1997. Clathrates — Computer programs to calculate fluid inclusion $v-X$ properties using clathrate melting temperatures. Comput. Geosci. 23, 1–18.

Benison, K.C., Goldstein, R.H., Wopenka, B., Burruss, R.C., Pasteris, J.D., 1998. Extremely acid Permian lakes and ground waters in North America. Nature 392, 911–914.

Bény, C., Feofanov, A., 1993. New data on fluid inclusions obtained with the help of a new micro-Raman confocal image spectrometer. Arch. Mineral. 49 (1), 27–28.

Bény, C., Guilhaumou, N., Touray, J.-C., 1982. Native-sulphur-bearing fluid inclusions in the CO_2–H_2S–H_2O–S system — microthermometry and Raman microprobe (MOLE) analysis — thermochemical interpretations. Chem. Geol. 37, 113–127.

Bergman, S.S., Dubessy, J., 1984. CO_2–CO fluid inclusions in a composite peridotite xenolith: implications for upper mantle oxygen fugacity. Contrib. Mineral. Petrol. 85, 1–13.

Bischoff, W.D., Sharma, S.K., Mackenzie, F.T., 1985. Carbonate disorder in synthetic and biogenic magnesian calcites: a Raman spectral study. Am. Mineral. 70, 581–589.

Bodnar, R.J., Szabó, Cs., Shilobreeva, S.N., Newman, S., 1996. Quantitative analysis of H_2O–CO_2 fluid inclusions by Raman spectroscopy. PACROFI VI (Madison, Wisconsin). Abstracts.

Boiron, M.-C., Dubessy, J., 1994. Determination of fluid inclusion compositions: microanalytical techniques. In: De Vivo, B., Frezzotti, M.L. (Eds.), Fluid Inclusions in Minerals: Methods and Applications. Pontignano, Siena, pp. 45–71, Short Course of the IMA Working Group 'Inclusions in Minerals'.

Boiron, M.-C., Moissette, A., Cathelineau, M., Banks, D., Monnin, C., Dubessy, J., 1999. Detailed determination of paleofluid chemistry: an integrated study of sulphate-volatile rich brines and aqueo-carbonic fluids in quartz veins from Ouro Fino (Brazil). Chem. Geol. 154, 179–192.

Bühn, B., Rankin, A.H., Radtke, M., Haller, M., Knöchel, A., 1999. Burbankite, a (Sr,REE,Na,Ca)-carbonate in fluid inclusions from carbonatite-derived fluids: identification and characterization using Laser Raman spectroscopy, SEM-EDX, and synchrotron micro-XRF analysis. Am. Mineral. 84, 1117–1125.

Burke, E.A.J., 1989. Quantitative laser Raman microspectrometry on fluid inclusions: an appraisal of five years of experience in Amsterdam. GéoRaman-89. Applications of Raman spectrometry to the earth sciences (Toulouse). p. 5, Abstracts.

Burke, E.A.J., 1998. New data on zircon from Matongo (Burundi). Aardk. Meded. KU Leuven 9, 17–20.

Burke, E.A.J., Lustenhouwer, W.J., 1987. The application of a multichannel laser Raman microprobe (Microdil-28®) to the analysis of fluid inclusions. Chem. Geol. 61, 11–17.

Burruss, R.C., Ging, T.G., Eppinger, R.G., Samson, I.M., 1992. Laser-excited fluorescence of rare-earth elements in fluorite: initial observations with a laser Raman microprobe. Geochim. Cosmochim. Acta 56, 2713–2723.

Cervelle, B., Moëlo, Y., 1990. Advanced microspectroscopy. Advanced Microscopic Studies of Ore Minerals. In: Jambor, J.L., Vaughan, D. (Eds.), Ottawa, MAC Short Course Handbook, vol. 17, pp. 379–408.

Cesare, B., Maineri, C., 1999. Fluid-present anatexis of metapelites at El Joyazo (SE Spain): constraints from Raman spectroscopy of graphite. Contrib. Mineral. Petrol. 135, 41–52.

Chou, I.-M., Pasteris, J.D., Seitz, J.C., 1990. High-density volatiles in the system C–O–H–N for the calibration of a laser Raman microprobe. Geochim. Cosmochim. Acta 54, 535–543.

Clocchiatti, R., Dhamelincourt, P., Massare, D., Tanguy, J.-C., Weiss, J., 1983. Les pyroclastes de l'éruption de 1669 de l'Etna: données physico-chimiques obtenues par l'étude des inclusions intraminérales. ECROFI (Orléans). p. 5, Abstracts.

Darimont, A., Burke, E.A.J., Touret, J.L.R., 1988. Nitrogen-rich metamorphic fluids in Devonian metasediments from Bastogne, Belgium. Bull. Minéral. 111, 321–330.

Da Silva, E., Roussel, B., 1982. Progrès récents en spectrométrie Raman (janvier 1981). Bull. Soc. Chim. Fr., Part I, 370–373.

Delhaye, M., Dhamelincourt, P., 1975. Raman microprobe and microscope with laser excitation. J. Raman Spectrosc. 3, 33–43.

Dhamelincourt, P., Bény, J.-M., Dubessy, J., Poty, B., 1979. Analyse d'inclusions fluides à la microsonde MOLE à effet Raman. Bull. Minéral. 102, 600–610.

Dhamelincourt, P., Schubnel, H.-J., 1977. La microsonde moléculaire à laser et son application à la minéralogie et la gemmologie: I. Rev. Gemmol. (Ass. Fr. Gemmol.) 52, (Septembre 1977).

Dong, G.Y., Pollard, P.J., 1997. Identification of ferropyrosmalite by laser Raman microprobe in fluid inclusions from metalliferous deposits in the Cloncurry district, NW Queensland, Australia. Mineral. Mag. 61, 291–293.

Dubessy, J., Boiron, M.-C., Moissette, A., Monnion, C., Sretenskaya, N., 1992. Determination of water, hydrates and pH in fluid inclusions by micro-Raman spectrometry. Eur. J. Mineral. 4, 885–894.

Dubessy, J., Geisler, D., Kosztolanyi, C., Vernet, M., 1983. The determination of sulphate in fluid inclusions using the MOLE Raman microprobe. Application to a Keuper halite and geochemical consequences. Geochim. Cosmochim. Acta 47, 1–10.

Dubessy, J., Moissette, A., Bakker, R.J., Frantz, J.D., Zhang, Y.-G., 1999. High-temperature Raman spectroscopic study of H_2O–CO_2–CH_4 mixtures in synthetic fluid inclusions: first

insights on molecular interactions and analytical implications. Eur. J. Mineral. 11, 23–32.

Dubessy, J., Pagel, M., Bény, J.-M., Christensen, H., Hickel, B., Kosztolanyi, C., Poty, B., 1988. Radiolysis evidenced by H_2-O_2- and H_2-bearing fluid inclusions in three uranium deposits. Geochim. Cosmochim. Acta 52, 1155–1167.

Dubessy, J., Poty, B., Ramboz, C., 1989. Advances in C–O–H–N–S fluid geochemistry based on micro-Raman spectrometric analysis of fluid inclusions. Eur. J. Mineral. 1, 517–534.

Fabre, D., Couty, R., 1986. Etude, par spectroscopie Raman, du méthane comprimé jusqu'à 3 kbar. Application à la mesure de pression dans les inclusions fluides contenues dans les minéraux. C. R. Acad. Sci. Paris, Ser. II 303, 1305–1308.

Fabre, D., Oksengorn, B., 1992. Pressure and density dependence of the CH_4 and N_2 lines in an equimolar CH_4/N_2 gas mixture. Appl. Spectrosc. 46, 468–471.

Frezzotti, M.L., Burke, E.A.J., De Vivo, B., Stefanini, B., Villa, I.M., 1992. Mantle fluids in pyroxenite nodules from Salt Lake Crater (Oahu Hawaii). Eur. J. Mineral. 4, 1137–1153.

Frezzotti, M.L., Burke, E.A.J., Ghezzo, C., 1995. CO/CO_2 fluid inclusions in aluminous metasedimentary xenoliths in siliceous lavas from Mt. Amiata (Tuscany, Italy). Bol. Soc. Esp. Mineral. 18-1, 80–81.

Frezzotti, M.L., Di Vincenzo, G., Ghezzo, C., Burke, E.A.J., 1994. Evidence of magmatic CO_2-rich fluids in peraluminous graphite-bearing leucogranites from Deep Freeze Range (northern Victoria Land, Antarctica). Contrib. Mineral. Petrol. 117, 111–123.

Fricke, A., Medenbach, O., Schreyer, W., 1990. Fluid inclusions, planar elements and pseudotachylites in the basement rocks of the Vredefort structure, South Africa. Tectonophysics 171, 169–183.

Gardiner, D.J., Graves, P.R. (Eds.), Practical Raman Spectroscopy. Springer, Berlin.

Garrabos, Y., Tufev, R., Le Neindre, B., Zalczer, G., Beysens, D., 1980. Rayleigh and Raman scattering near the critical point of carbon dioxide. J. Chem. Phys. 72, 4637–4651.

Griffith, W.P., 1974. Raman spectroscopy of minerals. In: Farmer, V.C. (Ed.), The Infrared Spectra of Minerals. Mineral. Soc. London Monogr., vol. 4, pp. 119–135.

Griffith, W.P., 1975. Raman spectroscopy of terrestrial minerals. In: Karr, C. Jr. (Ed.), Infrared and Raman Spectroscopy of Lunar and Terrestrial Minerals. Academic Press, New York, pp. 299–323.

Griffith, W.P., 1987. Advances in the Raman and infrared spectroscopy of minerals. In: Clark, R.J.H., Hester, R.E. (Eds.), Spectroscopy of Inorganic-based Materials. Wiley, New York, pp. 119–186.

Grishina, S., Dubessy, J., Kontorovich, A., Pironon, J., 1992. Inclusions in salt beds resulting from thermal metamorphism by dolerite sills (eastern Siberia, Russia). Eur. J. Mineral. 4, 1187–1202.

Guilhaumou, N., 1982. Analyse ponctuelle des inclusions fluides par microsonde moléculaire à laser (MOLE) et microthermométrie. Trav. Lab. Géol., Ec. Norm. Supér., Paris 14, 78 pp.

Guilhaumou, N., Dhamelincourt, P., Touray, J.-C., Barbillat, J., 1978. Analyse à la microsonde à effet Raman d'inclusions gazeuses du système N_2-CO_2. C. R. Acad. Sci. Paris, Sér. D 287, 1317–1319.

Guilhaumou, N., Jouaffre, D., Velde, B., Bény, C., 1988. Raman microprobe analysis on gaseous inclusions from the diagenetically altered Terres Noires (SE France). Bull. Minéral. 111, 577–585.

Hansteen, Th.H., Burke, E.A.J., 1990. Melt-mineral-fluid interaction in peralkaline silicic intrusions in the Oslo Rift, Southeast Norway: II. High-temperature fluid inclusions in the Eikeren-Skrim complex. Nor. Geol. Unders., Bull. 417, 15–32.

Herms, P., Schenk, V., 1992. Fluid inclusions in granulite-facies metapelites of the Hercynian ancient lower crust of the Serre, Calabria, Southern Italy. Contrib. Mineral. Petrol. 112, 393–404.

Hollister, L.S., Crawford, M.L. (Eds.), 1981. Fluid Inclusions: Applications to Petrology. Calgary, MAC Short Course Handbook, vol. 6, 304 pp.

Huizenga, J.M., Touret, J.L.R., 1999. Fluid inclusions in shear zones: the case of the Umwindsi shear zone in the Harare–Shamva–Bindura greenstone belt, NE Zimbabwe. Eur. J. Mineral. 11, 1079–1090.

Kerkhof, A.M. van den, 1987. The fluid evolution of the Harmsarvet ore deposit, central Sweden. Geol. Fören. Stockholm Förh. 109, 1–12.

Kerkhof, A.M. van den, 1988a. Phase transitions and molar volumes of $CO_2-CH_4-N_2$ inclusions. Bull. Minéral. 111, 257–266.

Kerkhof, A.M. van den, 1988. The system $CO_2-CH_4-N_2$ in fluid inclusions: theoretical modelling and geological applications. PhD Thesis, Vrije Universiteit Amsterdam, The Netherlands, 206 pp.

Kerkhof, A.M. van den, 1990. Isochoric phase diagrams in the systems CO_2-CH_4 and CO_2-N_2: application to fluid inclusions. Geochim. Cosmochim. Acta 54, 621–629.

Kerkhof, A.M. van den, 1991. Heterogeneous fluids in high-grade siliceous marbles of Pusula (SW Finland). Geol. Rundsch. 80, 248–258.

Kerkhof, A.M. van den, Kisch, H.J., 1993. CH_4-rich inclusions from quartz veins in the Valley-and-Ridge province and the anthracite fields of the Pennsylvania Appalachians — reply. Am. Mineral. 78, 220–224.

Kerkhof, A.M. van den, Olsen, S.N., 1990. A natural example of superdense CO_2 inclusions: microthermometry and Raman analysis. Geochim. Cosmochim. Acta 54, 895–901.

Kerkhof, A.M. van den, Touret, J.L.R., Maijer, C., Jansen, J.B.H., 1991. Retrograde methane-dominated fluid inclusions from high-temperature granulites of Rogaland, southwestern Norway. Geochim. Cosmochim. Acta 55, 2533–2544.

Kisch, H.J., Kerkhof, A.M. van den, 1991. CH_4-rich inclusions from quartz veins in the Valley-and-Ridge province and the anthracite fields of the Pennsylvania Appalachians. Am. Mineral. 76, 230–240.

Konnerup-Madsen, J., Dubessy, J., Rose-Hansen, J., 1985. Combined Raman microprobe spectrometry and microthermometry of fluid inclusions in minerals from igneous rocks of the Gardar province (south Greenland). Lithos 18, 271–280.

Konnerup-Madsen, J., Larsen, E., Rose-Hansen, J., 1979. Hydrocarbon-rich fluid inclusions in minerals from the alkaline Ilímaussaq intrusion, South Greenland. Bull. Minéral. 102, 642–653.

Kreulen, R., 1987. Thermodynamic calculations of the C–O–H system applied to fluid inclusions: are fluid inclusions unbiased samples of ancient fluids? Chem. Geol. 61, 59–64.

Larsen, R.B., Brooks, C.K., Bird, D.K., 1992. Methane-bearing, aqueous, saline solutions in the Skaergaard intrusion, east Greenland. Contrib. Mineral. Petrol. 112, 428–437.

Leng, J., Sharma, A., Bodnar, R.J., Pottorf, R.J., Vityk, M.O., 1998. Quantitative analysis of synthetic fluid inclusions in the H_2O–CH_4 system. PACROFI VII (Las Vegas, Nevada). Abstracts.

Luque, F.J., Pasteris, J.D., Wopenka, B., Rodas, M., Barrenechea, J.F., 1998. Natural fluid-deposited graphite — mineralogical characteristics and mechanisms of formation. Am. J. Sci. 298, 471–498.

McMillan, P., 1985. Vibrational spectroscopy in the mineral sciences. Rev. Mineral. 14, 9–63.

McMillan, P.F., 1989. Raman spectroscopy in mineralogy and geochemistry. Ann. Rev. Earth Planet. Sci. 17, 225–283.

McMillan, P.F., Hofmeister, A.M., 1988. Infrared and Raman spectroscopy. Rev. Mineral. 18, 99–159.

Mernagh, T.P., Hoatson, D.M., 1995. A laser-Raman microprobe study of platinum-group minerals from the Munni Munni layered intrusion, West Pilbara block, Western Australia. Can. Mineral. 33, 409–417.

Mernagh, T.P., Trudu, A.G., 1993. A laser Raman microprobe study of some geologically important sulphide minerals. Chem. Geol. 103, 113–127.

Mernagh, T.P., Wilde, A.R., 1989. The use of the laser Raman microprobe for the determination of salinity in fluid inclusions. Geochim. Cosmochim. Acta 53, 765–771.

Murata, K., Kawakami, K., Matsunaga, Y., Yamashita, S., 1997. Determination of sulfate in brackish waters by laser Raman spectroscopy. Anal. Chim. Acta 344, 153–157.

Murphy, P.J., Roberts, S., 1993. Micro-Raman spectroscopy of gas partitioning during clathrate formation: implications for microthermometric analysis. Arch. Mineral. 49 (1), 152.

Murphy, P.J., Roberts, S., 1995. Laser Raman spectroscopy of differential partitioning in mixed-gas clathrates in H_2O–CO_2–N_2–CH_4 fluid inclusions — implications for their microthermometry. Geochim. Cosmochim. Acta 59, 4809–4824.

Murphy, P.J., Roberts, S., 1997. Melting and nucleation behaviour of clathrates in multivolatile fluid inclusions — evidence of thermodynamic disequilibrium. Chem. Geol. 135, 1–20.

Norman, D.I., 1994. Analysis of SO_2 in fluid inclusions: fact or fiction. PACROFI V (Cuernavaca, Morelos, Mexico). p. 69, Abstracts.

Orange, D., Knittle, E., Farber, D., Williams, Q., 1996. Raman spectroscopy of crude oils and hydrocarbon inclusions: a feasibility study. In: Dyar, M.D., McCammon, C., Scaefer, M.W. (Eds.), Mineral Spectroscopy: A Tribute to Roger G. Burns. Geochem. Soc., Spec. Publ., vol. 5, pp. 65–81.

Pasteris, J.D., Kuehn, C.A., Bodnar, R.J., 1986. Applications of the laser Raman microprobe RAMANOR U-1000 to hydrothermal ore deposits: Carlin as an example. Econ. Geol. 81, 915–930.

Pasteris, J.D., Seitz, J.C., Morgan, G.B. VI, Wopenka, B., 1993. CH_4-rich inclusions from quartz veins in the Valley-and-Ridge province and the anthracite fields of the Pennsylvania Appalachians — discussion. Am. Mineral. 78, 216–219.

Pasteris, J.D., Wopenka, B., Seitz, J.C., 1988. Practical aspects of quantitative laser Raman microprobe spectroscopy for the study of fluid inclusions. Geochim. Cosmochim. Acta 52, 979–988.

Peretti, A., Dubessy, J., Mullis, J., Frost, B.R., Trommsdorf, V., 1992. Highly reducing conditions during Alpine metamorphism of the Malenco peridotite (Sondrio, northern Italy) indicated by mineral paragenesis and H_2 in fluid inclusions. Contrib. Mineral. Petrol. 112, 329–340.

Pinet, M., Smith, D.C., Lasnier, B., 1992. Utilité de la microsonde Raman pour l'identification non-destructive des gemmes (compilation d'une sélection représentative de leurs spectres Raman). Rev. Gemmol. (Ass. Fr. Gemmol.), 11–61, hors série Juin 1992.

Pironon, J., 1993. Estimation de la longueur de chaîne des hydrocarbures des inclusions fluides par spectrométrie Raman. C. R. Acad. Sci. Paris, Sér. II 316, 1075–1082.

Pironon, J., Sawatzki, J., Dubessy, J., 1992. NIR FT-Raman microspectroscopy of fluid inclusions: comparisons with VIS Raman and FT-IR microspectroscopies. Geochim. Cosmochim. Acta 55, 3885–3891.

Purcell, F.J., Etz, E.S., 1982. A new spectrograph with a multichannel optical detector for the Raman characterization of microparticles. In: Heinrich, K.F.J. (Ed.), Microbeam Analysis — 1982. San Francisco Press, San Francisco, pp. 301–306.

Roberts, S., Beattie, I., 1995. Micro-Raman spectroscopy in the earth sciences. In: Potts, P.J., Bowles, J.F.W., Reed, S.J.B., Cave, M.R. (Eds.), Microprobe Techniques in the Earth Sciences. Chapman & Hall, London, pp. 387–408.

Roedder, E., 1984. Fluid inclusions. Rev. Mineral. 12, 644 pp.

Roedder, E., 1990. Fluid inclusion analysis — prologue and epilogue. Geochim. Cosmochim. Acta 54, 495–507.

Rosasco, G.J., Roedder, E., 1979. Application of a new Raman microprobe spectrometer to nondestructive analysis of sulfate and other ions in individual phases in fluid inclusions in minerals. Geochim. Cosmochim. Acta 43, 1907–1915.

Rosasco, G.J., Roedder, E., Simmons, J.H., 1975. Laser-excited Raman spectroscopy for nondestructive partial analysis of individual phases in fluid inclusions in minerals. Science 190, 557–560.

Rosso, K.M., Bodnar, R.J., 1995. Microthermometric and Raman spectroscopic detection limits of CO_2 in fluid inclusions and the Raman spectroscopic characterization of CO_2. Geochim. Cosmochim. Acta 59, 3961–3975.

Saliot, P., Guilhaumou, N., Barbillat, J., 1982. Les inclusions fluides dans les minéraux du métamorphisme à laumontite-prehnite-pumpellyite des grès du Champsaur (Alpes du Dauphiné). Etude du mécanisme de circulation des fluides. Bull. Minéral. 105, 648–657.

Savary, V., Pagel, M., 1997. The effects of water radiolysis on local redox conditions in the Oklo, Gabon, natural fission reactors 10 and 6. Geochim. Cosmochim. Acta 61, 4479–4494.

Schrötter, H.W., Klöckner, H.W., 1979. Raman scattering cross-sections in gases and liquids. In: Weber, A. (Ed.), Raman Spectroscopy of Gases and Liquids. Springer-Verlag, Berlin, pp. 123–166.

Seitz, J.C., Pasteris, J.D., Chou, I-M., 1993. Raman spectroscopic characterization of gas mixtures: I. Quantitative composition and pressure determination of CH_4, N_2, and their mixtures. Am. J. Sci. 293, 297–321.

Seitz, J.C., Pasteris, J.D., Chou, I-M., 1996. Raman spectroscopic characterization of gas mixtures: II. Quantitative composition and pressure determination of the CO_2–CH_4 system. Am. J. Sci. 296, 577–600.

Seitz, J.C., Pasteris, J.D., Wopenka, B., 1987. Characterization of CO_2–CH_4–H_2O fluid inclusions by microthermometry and laser Raman microprobe spectroscopy: inferences for clathrate and fluid equilibria. Geochim. Cosmochim. Acta 51, 1651–1664.

Shepherd, T.J., Ayora, C., Cendón, D.I., Chenery, S.R., Moissette, A., 1998. Quantitative solute analysis of single fluid inclusions in halite by LA-ICP-MS and cryo-SEM-EDS: complementary microbeam techniques. Eur. J. Mineral. 10, 1097–1108.

Shepherd, T.J., Rankin, A.H., 1998. Fluid inclusion techniques of analysis. Rev. Econ. Geol. 10, 125–149.

Stein, C.L., Higgins, K.L., Morrison, R.L., 1989. Laser Raman microanalysis of fluid inclusions in halite. Eos 70, 1393.

Stephenson, D.A., 1974. Raman cross-sections of selected hydrocarbons and freons. J. Quant. Spectrosc. Radiat. Transfer 14, 1291–1301.

Sum, A.K., Burruss, R.C., Sloan, F.D., 1997. Measurement of clathrate hydrates via Raman spectroscopy. J. Phys. Chem. B 101, 7371–7377.

Thiéry, R., Vidal, J., Dubessy, J., 1994. Phase equilibria modelling applied to fluid inclusions: liquid-vapour equilibria and calculation of the molar volume in the CO_2–CH_4–N_2 system. Geochim. Cosmochim. Acta 58, 1073–1082.

Ting, W., Rankin, A.H., Woolley, A.R., 1994. Petrogenetic significance of solid carbonate inclusions in apatite of the Sukulu carbonatite, Uganda. Lithos 31, 177–187.

Touray, J.-C., Bény, C., Dubessy, J., Guilhaumou, N., 1985. Microcharacterization of fluid inclusions in minerals by Raman microprobe. Scanning Electron Microsc. 1985 1, 103–118.

Truchet, M., Delhaye, M., Bény, C., 1995. Identification of calcium carbonates (calcite, aragonite and vaterite) by Raman-Castaing microprobe — application to biomineralisations. Analusis 23, 516–518.

Wang, C.H., Wright, R.B., 1973. Effect of density on the Raman scattering of molecular fluids. I. A detailed study of the scattering polarization, intensity, frequency shift, and spectral shape of gaseous N_2. J. Chem. Phys. 59, 1706–1712.

White, W.B., 1975. Structural interpretation of lunar and terrestrial minerals by Raman spectroscopy. In: Karr, C. Jr. (Ed.), Infrared and Raman Spectroscopy of Lunar and Terrestrial Minerals. Academic Press, New York, pp. 325–358.

Winslow, D.M., Erickson, C.J., Tracy, R.J., Bodnar, R.J., 1991. Evidence for nitrogen-rich metamorphic fluids in the Central Maine Terrane of south-central Massachusetts. Geol. Soc. Am. Abstr. Program 23, 335.

Winter, C.J., Roberts, S., 1993. Laser Raman studies of low temperature hydrates produced in the highly saline fluids. Arch. Mineral. 49 (1), 246.

Wopenka, B., Pasteris, J.D., 1986. Limitations to quantitative analysis in of fluid inclusions in geological samples by laser Raman microprobe spectroscopy. Appl. Spectrosc. 40, 144–151.

Wopenka, B., Pasteris, J.D., 1987. Raman intensities and detection limits of geochemically relevant gas mixtures for a laser Raman microprobe. Anal. Chem. 59, 2165–2170.

Wopenka, B., Pasteris, J.D., 1993. Structural characterization of kerogens to granulite-facies graphite: applicability of Raman microprobe spectroscopy. Am. Mineral. 78, 533–557.

Wopenka, B., Pasteris, J.D., Freeman, J.J., 1990. Analysis of fluid inclusions by Fourier transform infrared and Raman microspectrometry. Geochim. Cosmochim. Acta 54, 519–533.